De-Gui Shu and Wen-Yu Chen*

Synthesis, structure, and *in vitro* anti-lung cancer activity on an In-based nanoscale coordination polymer

https://doi.org/10.1515/mgmc-2018-0027
Received June 4, 2018; accepted July 4, 2018; previously published online July 28, 2018

Abstract: Here, a new indium (In)-based coordination polymer $[In(hip)](DMF)_2(H_2O)_3$ (**1**, DMF = N,N-dimethylformamide) was successfully prepared by a solvothermal reaction of $In(NO_3)_3 \cdot 6H_2O$ and 5-hydroxyisophthalic acid (H_3hip) in a mixed solvent of DMF and H_2O with the presence of NaCl as a template. Complex **1** was characterized by elemental analysis (EA), single-crystal X-ray crystallography, and powder X-ray diffraction (PXRD), and the results reveal that complex **1** shows a two-dimensional (2D) grid-like network with considerable solvent accessible volume that was generated from the packing of the 2D layers via the AB pattern. Furthermore, complex **1** could be downsized into nanoscale particles with the aid of polyvinylpyrrolidone (PVP). In addition, the anticancer activities of **1** and the nanoscale **1** were probed via the 3-(4,5)-dimethylthiahiazo (-z-y1)-3,5-di-phenytetrazolium-romide (MTT) assay.

Keywords: downsizing; In(III)-based coordination polymer; MTT assay; X-ray structural analysis.

Introduction

The clinical success of cisplatin and its analogs has aroused broad interest in the investigation of new metal-based anticancer drugs over the past few decades (Doci et al., 1996; Wang and Lippard, 2005; Dasari and Bernard Tchounwou, 2014). Platinum-based anticancer drugs suffer from some serious drawbacks such as intrinsic or acquired resistance in some cancer types and undesirable side effects (Zhang et al., 2015). Therefore, there is an urgent need to develop novel metal-based anticancer therapeutic agents with different mechanisms of action that can overcome the aforementioned drawbacks of platinum-based chemotherapeutics.

The last few decades have witnessed the rapid development of a new kind of metal-organic crystalline material, called coordination polymers, which are composed of organic connection ligands and inorganic metal ions or clusters (Luo et al., 2015). Due to the endless possibilities in the selection of inorganic and organic building units and their highly ordered crystalline nature, coordination polymers have demonstrated many unique properties, such as high surface areas, clearly defined crystal structures, specially confined nanopore microenvironments, and uniform pore structures (Li et al., 2017a,b; Li and Li, 2018). To date, much effort has been devoted to the design and preparation of transition-metal coordination polymer materials because these metal elements are physiologically essential and have a function in endogenous oxidative DNA damage associated with aging and cancer (Wang et al., 2012). Metal ions that are essential for cells may become toxic at high concentrations because they can replace other important metals in enzymes (Chifotides and Dunbar, 2005). Accordingly, much of the literature has focused on the coordination of compound materials because of their good biocompatibility. Besides, coordination polymers can interact with DNA through noncovalent interactions, including intercalation and groove binding for large molecules and slot external electrostatic binding for cations. It has been previously reported that indium (In)-based coordination complexes showed promising antineoplastic activity against cancer cells *in vitro* (Bruijnincx and Sadler, 2008; Karmakar et al., 2013). Here, a new In-based coordination polymer was successfully prepared by a solvothermal reaction of $In(NO_3)_3 \cdot 6H_2O$ and 5-hydroxyisophthalic acid (Figure 1) in a mixed solvent of DMF and H_2O with the presence of NaCl as a template. The complex **1** was characterized by elemental analysis (EA), single-crystal X-ray crystallography, and powder X-ray diffraction (PXRD), and the anticancer activity of the nanoscale **1** was also evaluated using the MTT assay.

***Corresponding author: Wen-Yu Chen,** Department of Respiratory, The First Hospital of Jiaxing, Jiaxing 314001, Zhejiang, China, e-mail: wenyu_chen011@163.com
De-Gui Shu: Department of Respiratory, Sir Run Run Shaw Hospital, College of Medicine, Zhejiang University, Hangzhou 310016, Zhejiang, China

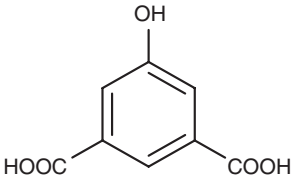

Figure 1: The chemical drawings for the H_3hip linkers employed in this study.

Table 1: Crystallographic parameters for compound **1**.

Formula	$C_{16}H_6InO_{10}$
*M*r	473.03
Crystal system	Monoclinic
Space group	*C*2/*c*
a/Å	14.530 (3)
b/Å	13.547 (3)
c/Å	12.274 (3)
α/°	90
β/°	97.06 (2)
γ/°	90
V/Å^3	2397.7 (9)
Z	4
Crystal size (mm^3)	0.21×0.16×0.11
D_{calc}/g cm^{-3}	1.310
μ(Mo Kα)/mm^{-1}	1.025
θ range/°	3.345–26.369
Reflections collected	5565
No. of unique data [*R*(int)]	2452 [0.0603]
No. of data with $I \geq 2\sigma(I)$	2034
R_1	0.0518
ωR_2 (all data)	0.1238
CCDC	1846968

Results and discussion

Molecular structure

The colorless crystals of **1** were obtained by the solvothermal reaction of $In(NO_3)_3 \cdot 6H_2O$ and 5-hydroxyisophthalic acid in a mixed solvent of DMF and H_2O with the presence of NaCl as a template. Bu and coworkers demonstrated that the addition of inorganic salts could effectively promote the crystallization of the In(III)-based coordination polymers (Zheng et al., 2010). X-ray crystallographic analysis revealed that **1** bears a two-dimensional (2D) grid-like network, crystallizing in the monoclinic C2/c space group (Table 1). There is one In(III) ion, one hip ligand and the disordered water, and DMF molecules in the molecular building unit. As shown in Figure 2A, the coordination surrounding of the eight-coordinated In(III) atom is finished by eight O atoms from four different carboxylic groups, resulting in a dodecahedral coordination environment. The In(III)-O bond distances are in the range of 2.173(2)–2.402(3) Å, and the mean In(III)-O bond distance is comparable to those of the reported similar complexes (Gándara et al., 2008; Panda et al., 2013). As for the hip ligand, its two carboxylic groups show μ_2-η^1-η^1 chelating fashion and connect with two adjacent In(III) ions along the axis to afford the hip-In(III)-hip chain, and then the 1D chains are further connected by the symmetry-related hip ligands in the b axis to afford the 2D-layered structure (Figure 2B). The window size for the grid-like window is 9.7×9.7 Å^2, and the solvent-accessible volume is 1037.9 Å^3, corresponding to 43.3% of the unit cell (Figure 2C). The topological analysis of one layer in complex **1** was also performed, and it revealed that complex **1** shows a typical 2D (4^4)-sql layered topology by considering the In(III) ions as four connected nodes and the hip ligand acting as two connected linkers. As shown in Figure 2D, complex **1** exhibits AA stacking double-layered framework along the ab plane, which might involve O-H···O and C-H···O hydrogen bond interactions among the hydroxy group, lattice DMF, and water molecules. These interactions not only consolidate the 2D structures but also make the three-dimensional (3D) supramolecular structures finally form.

To confirm the phase purity of complex **1**, the PXRD pattern was also recorded at room temperature. As shown in Figure 3, the PXRD patterns measured for the as-synthesized samples are in good agreement with the PXRD patterns simulated from the respective single-crystal X-ray data using the Mercury 3.1 program, demonstrating the phase purity of the products. In addition, the corresponding nanoscale coordination polymer of **1** was prepared by stirring the mixture of H_3hip, $In(CH_3COO)_2 \cdot 6H_2O$, and polyvinylpyrrolidone (PVP) in DMF and water. As shown in Figure 3B, a higher magnified scanning electron microscope (SEM) reveals that the average dimension of spherical particles is approximately 500±80 nm. Furthermore, the structure of the nanoscale **1** has been confirmed via the PXRD measurement, which reveals a similar framework as for complex **1**. In addition, the stability of the nanoscale **1** has also been confirmed via the PXRD measurement (Figure 3A).

Antitumor activity

The *in vitro* antitumor activities of H_3bip, **1**, and the nanoscale **1** against two human lung cancer cell lines A549 and NCI-H1299 were conducted by means of MTT tests. As shown in Figure 4, the H_3bip linker is compatible even after being incubated for 72 h at a high concentration

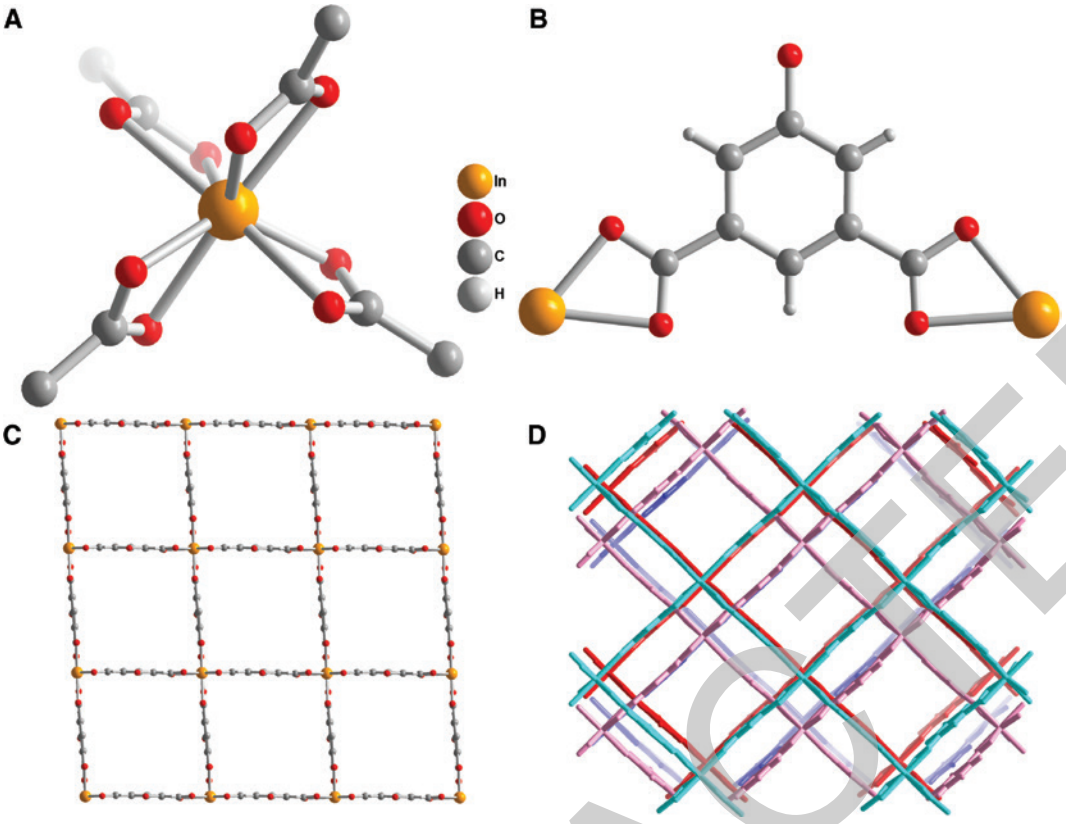

Figure 2: The structural characters for **1**.
(A) View for the atoms that shape the coordination surrounding of In(III) ion, (B) view of connecting model of bip ligand in **1**, (C) the single 2D grid network of **1** (the H atoms are omitted for clarity), and (D) the AB packing 2D layered network of **1**.

of 80 μg/mL with more than 90% cells still alive, indicating that the H_3bip ligand shows no obvious antitumor activity. In comparison, compound **1** and the nanoscale **1** exhibit potent cytotoxicities against the two cancer cell lines. It could be observed that more than 60% cancer cells are killed at the 40 μg/mL of the two complexes, and furthermore an increase of the concentration of the two complexes could lead to more cancer cell death, indicating that the cytotoxicities of these complexes are dose dependent. Compared with **1**, the nanoscale **1** shows more cell death under the same concentration, indicating that the antitumor activity of **1** is greatly enhanced by

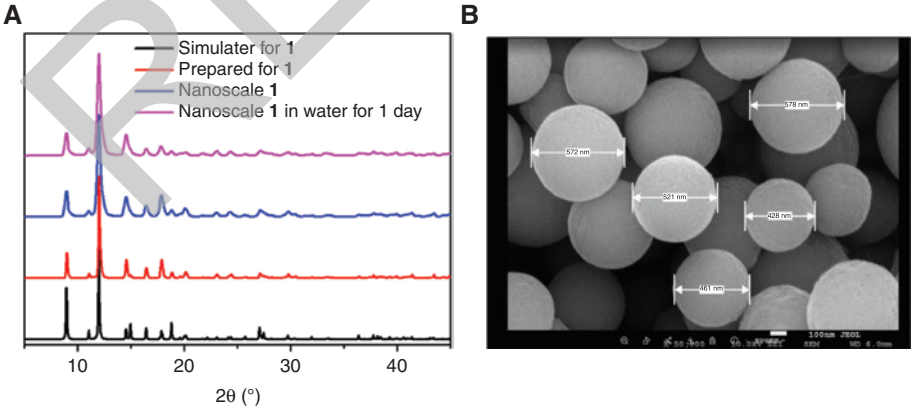

Figure 3: The PXRD patterns and SEM image for **1**.
(A) The PXRD patterns for **1** and (B) the SEM image of sphere morphology for the nanoscale **1**.

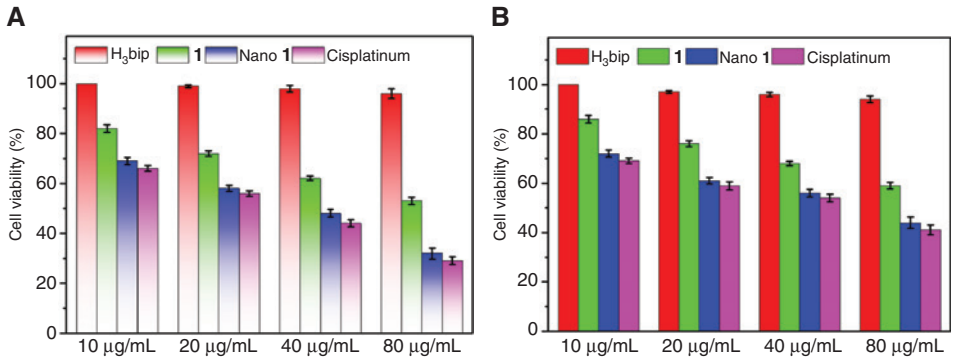

Figure 4: The MTT assay results for **1**.
Growth inhibitory effects of the H_3bip ligand, **1**, and the nanoscale **1** against the (A) A549 and (B) NCI-H1299 cell lines.

downsizing into nanoparticles. Although the underlying antitumor mechanism of the complexes is still uncertain, these results are highly significant in the following aspects: the nanoscale **1** shows stronger anticancer activities than the microscale **1**, indicating that the nanoscale **1** might form a stronger interaction with the cancer cell body. To make a comparable study with other anticancer drug, we use the cisplatinum as the positive control. As shown in Figure 4, the nanoscale **1** could result in comparable cancer cell death with the anticancer drug cisplatinum, indicating the comparable anticancer activity.

Conclusion

In summary, a new In-based coordination polymer has been successfully prepared by a solvothermal reaction of $In(NO_3)_3 \cdot 6H_2O$ and 5-hydroxyisophthalic acid (H_3hip) in a mixed solvent of DMF and H_2O with the presence of NaCl as template. The single-crystal X-ray crystallography result reveals that complex **1** shows a 2D grid-like network with a considerable solvent accessible volume that is generated from the packing of the 2D layers via the AB pattern. Furthermore, complex **1** could be downsized into nanoscale particles with the aid of PVP. In addition, the anticancer activities of **1** and the nanoscale **1** were probed using the MTT assay, which indicates that the anticancer activities of **1** were greatly enhanced via forming nanoparticles.

Experimental

Chemicals and instruments

All chemicals were of reagent grade and were used as commercially obtained from Bailingwei Chemical Technology Co. Ltd. (Beijing, China) without further purification. The In triacetate was bought from the Sigma-Aldrich reagent company (Tianjin, China). Elemental analyses (for C, H or N) were carried out on a Perkin-Elmer 240 elemental analyzer (PERKINELMER Company, Waltham, MA, USA). PXRD measurements were performed with a Bruker AXS D8 Advance instrument (Bruker Corporation, Karlsruhe, Germany). The Fourier-transform infrared spectroscopy (FTIR) spectra were recorded in the range 4000–400 cm^{-1} on a Nicolet 330 FTIR (Thermo Nicolet Corporation, Waltham, MA, USA) spectrometer using the KBr pellet method. The morphology of the as-prepared samples and the corresponding energy dispersive X-ray spectroscopy was obtained by a Hitachi S-4800 field-emission SEM.

Preparation and characterization for [In(hip)] $(DMF)_2(H_2O)_3$ (1)

A mixture of hip (10 mg, 0.05 mmol), $In(NO_3)_3 \cdot 6H_2O$ (41 mg, 0.1 mmol), and NaCl (10 mg) was dissolved in 2 mL of mixed solvents of DMF and H_2O (v/v = 3:1). After ultrasonication at room temperature for 10 min, the glass tube was sealed and placed in an oven and slowly heated from room temperature to 110°C over 10 h, kept at 110°C for 50 h, and then slowly cooled to 30°C for 800 min. The colorless crystals were collected and dried in air. (Yield: 60%, based on the hip ligand.) Anal calc found: for $C_{14}H_{23}InN_2O_{10}$: C, 34.03 (33.96); H, 4.69 (4.81); N, 5.67 (5.52)%. IR (KBr): ν (cm^{-1}) = 3507 (s), 3179 (m), 3078 (w), 2929 (w), 1664 (s), 1381 (s), 1274 (s), 1097 (s), 789 (s), 718 (s), 655 (m).

Preparation and characterization for the nanoscale 1

$In(CH_3COO)_3 \cdot H_2O$ (30 mg, 0.1 mmol) was dissolved in DMF (3 mL) and added to a mixture of PVP aqueous solution (11.2 mg, 1.5 mL). After a few minutes of stirring, H_3hip (10 mg, 0.05 mmol) was added to this solution. The obtained solution was mixed under vigorous stirring for 2 h at room temperature. Afterwards, it was left overnight at 110°C. The mixtures were precipitated with 10 mL acetone to yield white suspension, isolated by centrifugation at 4000 rpm (3700 *g*) for 15 min. After removal of the supernatant, the particles were washed with ethanol (100 mL) several times. The ethanol suspension was centrifuged again for 15 min at 4000 rpm (3700 *g*), and white powders were obtained.

Structural determination of 1 via X-ray diffraction

Single crystals of **1** with appropriate dimension were chosen under an optical microscope and quickly coated with high-vacuum grease (Dow Corning Corporation) before being mounted on a glass fiber for data collection. Data were collected on a Bruker Apex II Image Plate single-crystal diffractometer with graphite-monochromated Mo Kα radiation source ($\lambda = 0.71073$ Å) operating at 50 kV and 30 mA. All absorption corrections were applied using the multiscan program SADABS. In all cases, the highest possible space group was chosen. All structures were solved by direct methods using SHELXS-97 and refined on F^2 by full-matrix least-squares procedures with SHELXL-97. For the disordered nature of the lattice DMF and water molecules, they could not be figured out from the structural model, so their electrons were removed from the HKL file using the squeeze manipulation in the software PLATON.

Antitumor activity

The 3×10^4 cancer cells per well were seeded in 96-well plates (TPP, St. Louis, MO, USA) in a complete medium and kept at 37°C in a humidified atmosphere of 5% CO_2 and incubated for 12 h prior to experimental treatments. Then, the cells were treated with various concentrations of **1** and solely 0.5% dimethyl sulfoxide (DMSO)/H_2O solution for 24 and 48 h, respectively. Then, the culture medium was removed and refreshed with 200 μL of fresh complete medium containing 20 μL of MTT [5 mg/mL in phosphate buffered saline (PBS)] for further 4 h of incubation. After the supernatant was removed, 150 μL/well of DMSO was added to dissolve the purple formazan crystals. The absorbance was read on a Thermo Scientific Varioskan Flash at 570 nm. Nontreated cells [in Dulbecco's Modified Eagle's Medium (DMEM)] were used as the control, and the relative cell viability [mean % ± standard deviation (SD), n = 3] was expressed as OD sample/OD control × 100%.

References

Bruijnincx, P. C.; Sadler, P. J. New trends for metal complexes with anticancer activity. *Curr. Opin. Chem. Biol.* **2008**, *12*, 197–206.

Chifotides, H. T.; Dunbar, K. R. Interactions of metal – metal-bonded antitumor active complexes with DNA fragments and DNA. *Acc. Chem. Res.* **2005**, *38*, 146–156.

Dasari, S.; Bernard Tchounwou, P. Cisplatin in cancer therapy: molecular mechanisms of action. *Eur. J. Pharmacol.* **2014**, *740*, 364–378.

Doci, R.; Zucali, R.; La Monica, G.; Meroni, E.; Kenda, R.; Eboli, M.; Lozza, L. Primary chemoradiation. Therapy with fluorouracil and cisplatin for cancer of the anus: results in 35 consecutive patients. *J. Clin. Oncol.* **1996**, *14*, 3121–3125.

Gándara, F.; Gomez-Lor, B.; Gutiérrez-Puebla, E.; Iglesias, M.; Monge, M. A.; Proserpio, D. M.; Snejko, N. An. Indium layered MOF as recyclable Lewis acid catalyst. *Chem. Mater.* **2008**, *20*, 72–76.

Karmakar, T.; Kuang, Y.; Neamati, N.; Baruah, J. B. Cadmium complexes and cocrystals of indium complexes of benzothiazole derivatives and anticancer activities of the cadmium complexes. *Polyhedron* **2013**, *54*, 285–293.

Li, J.; Li, J. T. A luminescent porous metal-organic framework with Lewis basic pyridyl sites as a fluorescent chemosensor for TNP detection. *Inorg. Chem. Comm.* **2018**, *89*, 51–54.

Li, J.; Ji, X. H.; Li, J. T. Two new inorganic anions directed Zn(II)-tetrazole frameworks: syntheses, structures and photoluminescent properties. *J. Mol. Struct.* **2017a**, *1147*, 22–25.

Li, J. T.; Li, J.; Song, L. M.; Ji, X. H. Microporous metal-organic framework with 1D helical chain building units: synthesis, structure and gas sorption properties. *Inorg. Chem. Comm.* **2017b**, *83*, 88–91.

Luo, X.; Sun, L.; Zhao, J.; Li, D. S.; Wang, D.; Li, G.; Huo, Q.; Liu, Y. Three metal-organic frameworks based on binodal inorganic building units and hetero-O, N donor ligand: solvothermal syntheses, structures, and gas sorption properties. *Cryst. Growth Des.* **2015**, *15*, 4901–4907.

Panda, T.; Kundu, T.; Banerjee, R. Structural isomerism leading to variable proton conductivity in indium(iii) isophthalic acid based frameworks. *Chem. Commun.* **2013**, *49*, 6197–6199.

Wang, D.; Lippard, S. J. Cellular processing of platinum anticancer drugs. *Nat. Rev. Drug Discov.* **2005**, *4*, 307–320.

Wang, K.; Ma, X.; Shao, D.; Geng, Z.; Zhang, Z.; Wang, Z. Coordination-induced assembly of coordination polymer submicrospheres: promising antibacterial and in vitro anticancer activities. *Cryst. Growth Des.* **2012**, *12*, 3786–3791.

Zhang, W.; Li, Y.; Sun, J.-H.; Tan, C.-P.; Ji, L.-N.; Mao, Z.-W. Supramolecular self-assembled nanoparticles for chemo-photodynamic dual therapy against cisplatin resistant cancer cells. *Chem. Commun.* **2015**, *51*, 1807–1810.

Zheng, S. T.; Bu, J. T.; Li, Y.; Wu, T.; Zuo, F.; Feng, P.; Bu, X. Pore space partition and charge separation in cage-within-cage indium-organic frameworks with high CO_2 uptake. *J. Am. Chem. Soc.* **2010**, *132*, 17062–17064.